Catalysis Today 158 (2010) 504–509

Contents lists available at ScienceDirect

Catalysis Today

journal homepage: www.elsevier.com/locate/cattod

Catalytic cracking of n-heptane over HZSM-5 catalysts with the activation of lattice oxygen

Xiaoyan Hu, Chunyi Li*, Chaohe Yang

State Key Laboratory of Heavy Oil Processing, China University of Petroleum, Qingdao 266555, Shandong, PR China

ARTICLE INFO

Article history:
Available online 6 September 2010

Keywords:
Paraffin
HZSM-5
Light olefins
V_2O_5/Al_2O_3
Lattice oxygen
Activation

ABSTRACT

Paraffin, one of the major components of straight-run naphtha, is relatively inert compared with olefin, which poses a difficulty for catalytic cracking of naphtha. The present study proposed introducing lattice oxygen into previous HZSM-5 catalyst system to improve conversion and light olefin selectivity. Vanadium oxide based catalyst was prepared separately as the lattice oxygen provider and then mixed with HZSM-5 catalyst for evaluation in a fixed-bed reactor using n-heptane as model compound. The results demonstrated that conversion of reactant increased from ~51% to ~59% by replacing 20% of HZSM-5 catalyst with V_2O_5/Al_2O_3; depending on different location of V_2O_5/Al_2O_3 relative to HZSM-5 catalyst in the reactor, conversion and product distribution varied significantly, while the addition of pure alumina did not have such an effect. Besides, water was formed in liquid products accompanied by reduction of V^{5+} during the reaction, as revealed by FT-IR and XRD results, respectively; the oxidized V^{5+} seemed to have greater capability in promoting conversion of n-heptane. Therefore, it was concluded that n-heptane could be activated by lattice oxygen provided by oxidized vanadia before further cracking over acidic sites in HZSM-5 catalyst.

1. Introduction

The production of light oelfins, especially propylene, is of growing interest, for they are of great importance in petrochemical industry. One of the important sources of them is fluid catalytic cracking (FCC) process, and either special catalysts or technologies [1–6] were investigated for increasing yields of the light olefins. TMP [3] (two-stage riser FCC for maximization of propylene) process was designed for maximizing propylene yield on FCC unit, by recycling light gasoline fraction; it was found that paraffin of light gasoline fraction can hardly be converted and remained in the products [3,7,8].

What's more, current catalytic cracking of naphtha, which is supposed to be desirable alternative to replace steam cracking technology in producing light alkenes, mostly ascribed to its advantages in low energy consumption and favorable product distribution [9], is also confronted with difficulty in paraffin transformation. There is a contradiction between conversion level and product distribution under industrial operation condition [10]. In addition, cracking of paraffin usually lead to lower light alkene selectivity compared with the cracking of olefin.

Paraffin, one of major constituents of light straight-run naphtha, is well known for its inertness, and methods were studied to activate paraffin molecule, or increase reactivity of paraffin reactant. It was reported that introduction of gas phase oxygen would result in higher conversion and light olefins yield compared with thermal cracking, and it maybe due to easiness of C–H bond rupture activated by oxygen and the depression of activation energy with oxygen participation [11]. However, the presence of gas phase oxygen would easily lead to deep oxidation reactions producing higher amounts of CO_x. The employment of lattice oxygen instead of molecule oxygen may probably smooth the problem of total oxidation, for it is generally believed that lattice oxygen is the active species for selective oxidation [12]. López Nieto et al. [13] and Busca [14] had suggested that olefin, alkoxide or some other O-insertion species may form as intermediates during oxidative dehydrogenation of light alkanes. Both olefin and O-containing compound are of relatively easier cracking property, as we have confirmed in our previous study.

Therefore, we intended to introduce catalyst containing lattice oxygen into previous cracking system, in order to increase reactivity of paraffin in the present study. Vanadia-based catalysts were employed as lattice oxygen supplier, for its wide application in selective or partial oxidation reactions [15–21].

---

* Corresponding author at: State Key Laboratory of Heavy Oil Processing, China University of Petroleum, No. 66, Qingdao 266555, Shandong, PR China.
Tel.: +86 532 86981862.
E-mail addresses: hxy.hope@gmail.com (X. Hu), chyli@upc.edu.cn (C. Li), statekeylab@upc.edu.cn (C. Yang).

0920-5861/$ – see front matter © 2010 Elsevier B.V. All rights reserved.
doi:10.1016/j.cattod.2010.07.028

2. Experiments

2.1. Catalyst preparation

In this work, alumina supported vanadia catalyst (V_2O_5/Al_2O_3) and P/HZSM-5/Kaolin catalysts were prepared, separately, and the two catalysts were physically mixed proportionately for test, in order to avoid vanadia's negative effects on zeolite.

The procedure for preparation of V_2O_5/Al_2O_3: vanadyl oxalate solution was prepared by mixing vanadium pentoxide with excessive amounts of oxalic acid, adding a given amount of deionized water to make certain concentration of vanadyl oxalate solution. V_2O_5/Al_2O_3 catalyst was obtained by impregnating γ-Al_2O_3 with the above solution, followed by drying at 120 °C and calcination at 600 °C. Finally, the obtained sample was crushed and sieved to give catalyst particle size of 0.088–0.200 mm.

P/HZSM-5/Kaolin catalyst was obtained by semi-synthetic method using HZSM-5 (Si/Al = 38) as the active components. The sample was all undergone hydrothermal treatment at 780 °C for 4 h with water flow rate of 0.6 ml/min before catalytic test to make its performances close to equilibrium state.

2.2. Characterization results

TG-DTA analyses were performed on DTU-2A differential thermal gravimetric analyzer. Typically, 30 mg catalyst was put on the sample holder inside an aluminum crucible, using α-Al_2O_3 as reference. The sample was submitted to a linear rise of temperature from room temperature to 1000 °C, with heating rate of 10 °C/min.

Physical phase of the samples were determined by XRD technique on a Rigaku D/Max RB diffractometer using Cu Kα radiation, and operated at 40 kV and 40 mA, with a scanning speed of 10°/min.

The specific surface area and pore structure property of samples were determined by N_2 adsorption–desorption measurements carried out at 77 K on Micromeritics accelerated surface area and porosimetry analyzer (ASAP 2010).

The FT-IR spectra of organic liquid product were determined on Nicolet Nexus Fourier transform instrument and recorded in the range of 4000–400 cm^{-1}.

2.3. Catalytic test

The catalysts' performances in cracking of n-heptane were measured under atmosphere pressure in a conventional fixed-bed reactor at 570 °C. Catalysts with the particle size of 0.088–0.200 mm of 5 g were loaded into a stainless steel reactor. The catalysts were pre-purged by nitrogen gas to remove adsorbed water prior to reaction; n-heptane of 0.78 g was introduced into the reactor by nitrogen gas of 30 ml/min via switching six-way plug valve.

Influences of reaction time were also evaluated at similar conditions, except that continuous reaction was adopted. The flow rate of n-heptane was 2 ml/min.

The composition of gaseous products were analyzed by Varian 3800 chromatography, with a TCD detector coupled with 5A and 13X molecular sieve capillary column to analyze content of hydrogen, nitrogen and carbon oxide, and a FID detector coupled with an Al_2O_3 PLOT capillary column to determine the composition of hydrocarbon. Analysis of organic liquid products was carried out at HP5890 chromatography with FID detector and PONA capillary column by three-stage temperature programmed analyzing method.

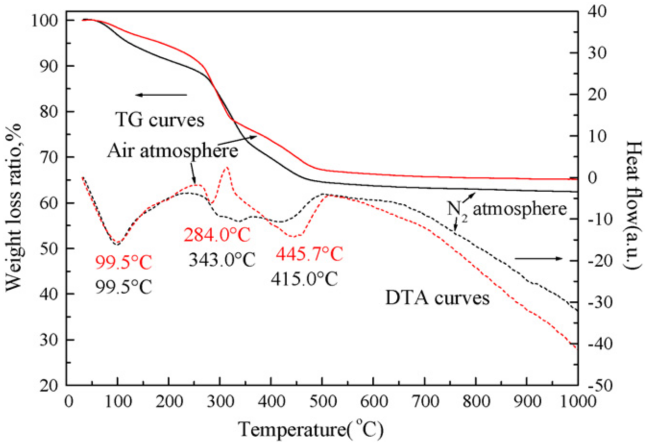

Fig. 1. The TG-DTA plots of V_2O_5/Al_2O_3 precursor.

3. Results and discussion

3.1. Physicochemical properties of catalysts

V_2O_5/Al_2O_3 catalyst was prepared by impregnation with vanadyl oxalate solution as stated in Section 2.1. As we have already known, oxalic acid is a medium strong reducing agent and easily leads to reduction of V^{5+} to V^{4+} during the preparation of V_2O_5/Al_2O_3 precursor. TG-DTA analysis of the catalyst precursor under different atmospheres is shown in Fig. 1. It was observed that there were three stages of weight loss on the TG curves, which corresponded to different endothermic peaks on the DTA curves. They could be attributed to dehydration of adsorbed water, decomposition of excessive oxalic acid and VOC_2O_4, respectively. Overall, weight loss of the precursor under air atmosphere was less than that under nitrogen atmosphere, suggesting oxidization of V^{4+} to V^{5+} in the presence of oxygen. DTA analysis had also been carried out with the mixture of P/HZSM-5/Kaolin and V_2O_5/Al_2O_3 catalyst particles under N_2 atmosphere, in order to find whether there was any endothermic or exothermic peak that might be indicative of phase transformation or solid-state interaction between the two catalysts. The results (not shown) revealed that only a small dehydration peak at ~100 °C was observed.

The specific surface area and pore structure property of γ-alumina support, hydrothermally treated P/HZSM-5/Kaolin and V_2O_5/Al_2O_3 catalyst are tabulated in Table 1. The BET surface area of HZSM-5 catalyst obtained by N_2 physisorption at 77 K, was found to be 211 m^2/g with total pore volume of 0.26 cm^3/g. Compared with the alumina support, impregnation of vanadia led to significant decrease in surface area and pore volume, indicating that penetration of surface vanadia species into the pores of alumina.

XRD patterns of 15 wt.% V_2O_5/Al_2O_3 catalyst exhibited only the lines of spinel phase of γ-Al_2O_3, as demonstrated by Fig. 2, indicating well dispersion of the vanadia on alumina support. Compared with the support, intensity of the lines ascribed to alumina in

Table 1
Texture property of catalysts.

Catalyst	S_{BET} (m^2/g)	V pore (cm^3/g)	V micro (cm^3/g)	V meso (cm^3/g)
P/HZSM-5/Kaolin	211.0	0.26	0.12	0.14
Al_2O_3	167.0	0.28	–	0.28
15 wt.% V_2O_5/Al_2O_3	142.3	0.24	–	0.24

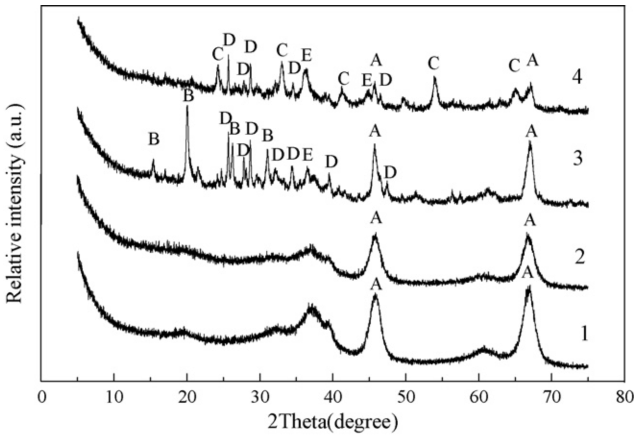

Fig. 2. X-ray diffraction patterns of V_2O_5/Al_2O_3 catalysts.

the V_2O_5/Al_2O_3 catalyst decreased, and it suggested a decline in crystallinity of alumina in the samples. In order to obtain information related to changes of vanadia species during the reaction, XRD patterns of the fresh and used 50 wt.% V_2O_5/Al_2O_3 were compared. Besides the phase of alumina, lines ascribed to V_2O_5 and $AlVO_4$ phase were detected on the fresh sample, and the latter indicated that strong interaction existed between vanadia and alumina support. It seemed possible to suggest that, consistent with the literatures [22–25], high vanadia loadings easily led to low vanadium dispersion, promoting formation of $AlVO_4$ phase and bulk-like V_2O_5. The disappearance of V_2O_5 phase and formation of V_2O_3 in catalyst after reaction at 570 °C demonstrated a reduction of $V^{5+} \rightarrow V^{3+}$ process. However, $AlVO_4$ phase remained with decreasing intensity and the lines ascribed to AlV_2O_4 were observed for the used sample suggesting more difficulty for reduction of $AlVO_4$ than V_2O_5 crystalline. Kanervo et al. [23] observed that $AlVO_4$ remained after reduction at 480 °C and disappeared after reduction at 650 °C, and thus concluded that crystalline $AlVO_4$ was reduced at temperature between 480 °C and 650 °C. It was reported that much higher reduction temperature of $AlVO_4$ was attributed to its lower accessibility compared with well-dispersed vanadia species, and it was supposed to be the main reason for lower activity of catalyst with high vanadia loading.

Fig. 3 shows FT-IR spectra of n-heptane reactant and liquid products obtained on different catalysts. Distinct bands at 2959, 2925, 2873 and 2858 cm^{-1} were assigned to the C–H stretching vibrations of n-heptane, and bands at 1467, 1378 cm^{-1} were due to C–H bending vibrations, as shown in Fig. 3a. The intensity of these bands decreased after reaction, especially for the mixed catalyst, indicating that stronger cracking ability of P/HZSM-5/Kaolin, as we expected. New bands appeared at 3028, 1605, 1495 and 694 cm^{-1} in liquid product obtained on V_2O_5/Al_2O_3, were most probably attributed to formation of aromatics. These bands were extremely weak in liquid product for the mixed catalysts, indicating that the V_2O_5/Al_2O_3 promoted aromatization. Besides, a weak and broad band at 3440 cm^{-1} was found in the products, and it was most probably assigned to the existence of small quantity of dissolved water caused by the presence of V_2O_5/Al_2O_3.

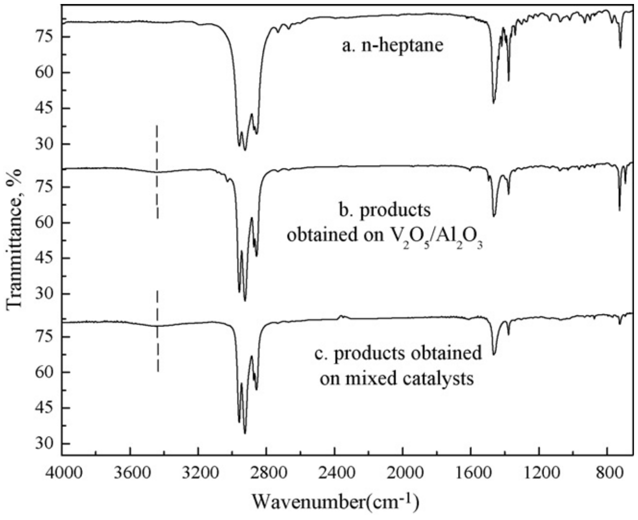

Fig. 3. FT-IR spectra of n-heptane and organic liquid product obtained on V_2O_5/Al_2O_3 and mixed catalysts.

3.2. The influences of V_2O_5/Al_2O_3 introduction on catalytic cracking of n-heptane

Vanadium atoms can exist in different forms of oxidation states, varying from 2 to 5. The easy conversion between oxides of different stoichiometry and formation of oxygen vacancies enables the oxide to function as catalyst in selective oxidation [26]. Therefore, V_2O_5/Al_2O_3 catalyst was prepared as lattice oxygen supplier in the present study.

The influences of V_2O_5/Al_2O_3 introduction on the performances of catalytic cracking of n-heptane over P/HZSM-5/Kaolin catalyst were investigated by single pulse reaction. The results are summarized in Table 2. On hydrothermally treated P/HZSM-5/Kaolin catalyst, conversion of n-heptane achieved 51.32%, with C_3 (propane and propylene) and C_4 (butane and butylene) as main gaseous products and no carbon oxide was observed in the products. Plenty of aromatic compounds were formed with total yield of 2%. Besides aromatics, other hydrocarbon products in range of C_5–C_{10} were also formed in the liquid products, corroborating complexity of reaction network, which included cracking, dehydrogenation and aromatization, etc. Comparatively, conversion of n-heptane over pure alumina was much lower, giving a value of 23.60%; however, hydrogen production was significantly higher, most probably attributed to abundant Lewis acidic sites of alumina. It was believed that Bronsted acid sites and Lewis acid sites differed greatly in dehydrogenation ability, and the former mainly catalyzed C–C cracking, while the latter exhibited a strong preference for C–H activation, according to the results observed with Lewis acid Ga sites in ZSM-5 zeolite [27]. The catalytic activity of V_2O_5/Al_2O_3 was even lower than alumina, giving conversion of 18.41%. Impregnation of vanadia over alumina led to blockage of at least some of the Lewis acid sites on the surface of alumina, and that was supposed to be the main reason for decrease in catalysts' activity. Besides, the product distribution on V_2O_5/Al_2O_3 exhibited characteristics of thermal cracking, high yield of dry gas relative to liquefied petroleum gas. This was in accordance with that reported in literature [28], which reported that presence of metal oxide catalysts did not change product distribution of thermal cracking and only the initiation reaction was promoted. Thus the P/HZSM-5/Kaolin was the main activity contributor in the mixed catalysts.

In addition to the P/HZSM-5/Kaolin, V_2O_5/Al_2O_3 and alumina alone, the mixture of V_2O_5/Al_2O_3 and P/HZSM-5/Kaolin catalysts were charged into the reactor with different positions, as shown by Fig. 4d–f. The total mass amount of catalysts was kept identical in each case. The reactant was carried into the reactor by nitrogen gas downwardly. Different distributions of the two catalysts in reactor resulted in their different interaction sequences with the reactant. It was noticed that, compared with the P/HZSM-5/Kaolin catalyst alone, conversion on the mixed catalysts of V_2O_5/Al_2O_3 above P/HZSM-5/Kaolin (No d) and well-distributed mixture of them (No f) was obviously higher by about 16%. Actually, addition of the V_2O_5/Al_2O_3 decreased the number of acidic sites of P/HZSM-

Table 2
Influences of catalyst distribution in reactor on catalytic performances.

No		a	b	c	d	e	f	g
Conversion, m%		51.32	18.41	23.60	59.98	50.98	58.34	47.29
Yield, m %	H_2	0.18	1.30	1.52	0.85	0.65	0.58	0.52
	CH_4	0.39	0.32	0.37	0.54	0.60	0.50	0.37
	C_2H_6	1.86	0.23	0.19	1.62	2.20	1.79	1.77
	C_2H_4	3.40	0.13	0.22	3.19	2.09	2.91	3.29
	C_3H_8	8.54	0.13	1.17	5.80	6.60	6.41	7.04
	C_3H_6	7.75	0.54	3.61	9.46	6.87	9.61	6.98
	C_4H_{10}	3.78	0.39	0.77	2.64	2.72	2.89	3.15
	C_4H_8	4.02	0.37	0.63	4.80	3.70	4.89	3.27
	CO	0	0.53	0.00	0.73	0.86	0.81	0.00
	CO_2	0	0.37	0.12	1.24	1.18	1.18	0.03
	Arene	2.00	1.29	1.35	5.97	4.15	3.96	1.86
	Dry gas	5.84	1.98	2.30	6.20	5.54	5.78	5.95
	LPG	24.10	1.43	6.18	22.71	19.89	23.8	20.44
Mole ratio	C_2H_4/C_2H_6	1.96	0.61	1.24	2.10	1.02	1.74	1.99
	C_3H_6/C_3H_8	0.95	4.35	3.23	1.71	1.09	1.57	1.04
	C_4H_8/C_4H_{10}	1.11	0.98	0.85	1.88	1.41	1.75	1.08
	C_3H_6/C_2H_4	1.52	2.77	10.94	1.98	2.19	2.20	1.41
	C_4H_8/C_2H_4	0.59	1.42	1.43	0.75	0.88	0.84	0.50

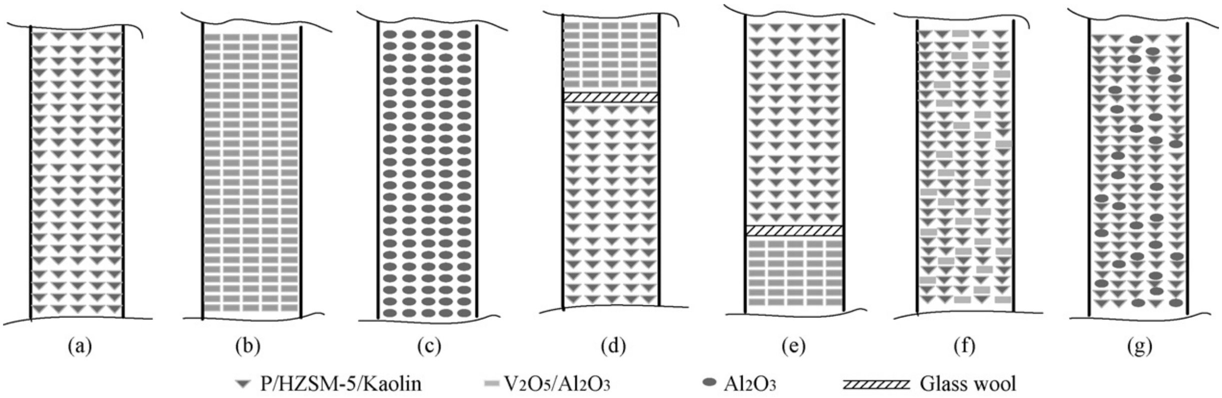

Fig. 4. Schematic diagram for catalysts of different distributions in fixed-bed reactor.

5/Kaolin for cracking, for total catalysts weight was kept constant in each test. In spite of that, conversion improved obviously, showing that V_2O_5/Al_2O_3 greatly improved the overall activity of the catalysts in the cases. However, things were much different in the mixed catalysts with V_2O_5/Al_2O_3 below P/HZSM-5/Kaolin (No e). Despite the same catalyst composition, catalytic performances differed greatly; conversion obtained on it was only 50.98%. It seemed that promotion effect of the V_2O_5/Al_2O_3 disappeared, or at least much weakened, by introducing the V_2O_5/Al_2O_3 under P/HZSM-5/Kaolin. What's more, product distribution also varied greatly in different cases. For example, introduction of V_2O_5/Al_2O_3 led to prominent higher yield of carbon oxide, hydrogen and aromatics, indicating more occurrences of oxidation, dehydrogenation and cyclization reactions in the presence of V_2O_5/Al_2O_3. Besides, addition of vanadia resulted in higher ratios of propylene/propane, butylene/butane, propylene/ethylene, and butylene/ethylene.

Performance of the homogeneous mixture of P/HZSM-5/Kaolin and alumina was also evaluated, as shown by No g. The conversion was much lower than that on pure P/HZSM-5/Kaolin catalyst, but selectivity to hydrogen and dry gas was higher, most probably attributed to Lewis acidic sites, as we have discussed above.

3.3. *Influences of time on stream on catalytic activity with and without V_2O_5/Al_2O_3*

Catalytic cracking of n-heptane was also carried out in a way of continuous reaction. The conversion of n-heptane over catalysts not containing and containing V_2O_5/Al_2O_3 was compared at different reaction times, as shown by Fig. 5. Generally, conversion of n-heptane decreased with increasing reaction time, as we expected. It was indicated that at the beginning of the reaction, the conversion of n-heptane was evidently higher on the mixed P/HZSM-5/Kaolin

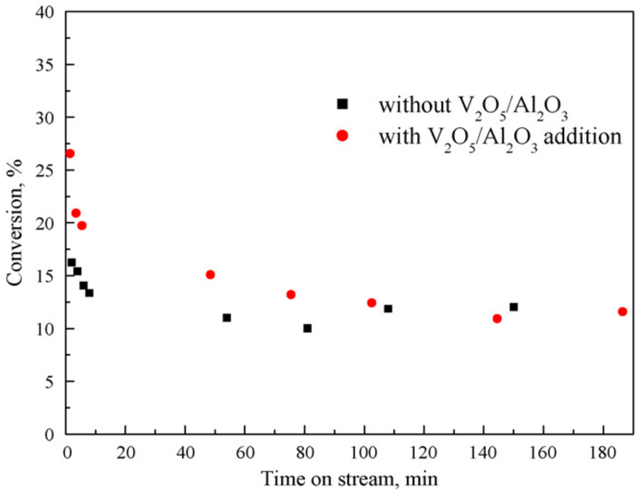

Fig. 5. Conversion of n-heptane over catalyst with and without vanadia catalyst as a function of time on stream.

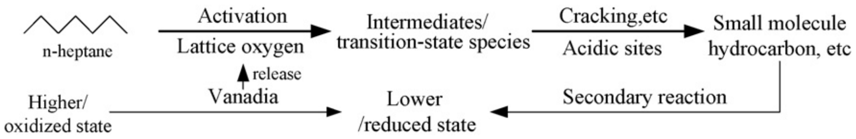

Fig. 6. Schematic diagram for supposed reaction pathways of n-heptane over mixed catalysts.

and V_2O_5/Al_2O_3 catalysts. With the prolonged reaction time, the advantage of catalytic activity of the mixed catalysts was weakened greatly. After about 90 min time on stream, the conversions on them were very close to each other. It was explained that after the consumption of accessible lattice oxygen, vanadia-based catalyst lost its ability in activation of reactant molecule. Therefore, the oxidized vanadia sites that can provide lattice oxygen, were supposed to be active sites in the V_2O_5/Al_2O_3 catalyst.

3.4. *Effects of regeneration*

The used mixed catalysts were regenerated and evaluated in fixed-bed reactor by intermittent reaction way. The results are compared with that of fresh sample and tabulated in Table 3. It was found that either activity or selectivity was obviously influenced by regeneration, and this makes it possible for cracking of n-heptane over the mixed P/HZSM-5/Kaolin and V_2O_5/Al_2O_3 catalysts to be operated in a circulated fluidized bed successively.

3.5. *Discussion*

In the present study, the data strongly suggested that lattice oxygen got involved in the reaction, for water and considerable amounts of carbon oxides were formed, besides, V^{5+} was reduced during the reaction, as revealed by the XRD results.

Compared with the hydrothermally treated P/HZSM-5/Kaolin and V_2O_5/Al_2O_3 alone, catalytic cracking of n-heptane over the mixture of them gave relatively higher conversion, indicating a synergistic co-action between them. What's more, different distribution of the two catalysts posed great influences on both conversion and product selectivity. It was found that the mixed catalysts with V_2O_5/Al_2O_3 located under P/HZSM-5/Kaolin was most unfavorable in terms of conversion. Combining with lattice oxygen involvement during the reaction and what has been reported previously [13,14,19,28,29], we concluded that lattice oxygen in V_2O_5/Al_2O_3 catalysts smoothed initiation reaction of n-heptane, which was supposed to be rate-determining step during the paraffin transformation process. As a result, those n-heptane molecules activated by V_2O_5/Al_2O_3 were easier to convert, or, it was much more effective for n-heptane to contact with V_2O_5/Al_2O_3 before P/HZSM-5/Kaolin. Compared with hierarchically distributed catalysts, the well-dispersed mixed catalysts was more convenient for intermediates activated by V_2O_5/Al_2O_3 to be transferred to acid sites in P/HZSM-5/Kaolin for further cracking, due to much closer distance between the two different active sites. In this case, the incidence of excessive dehydrogenation or over-oxidation reactions decreased, which resulted in lower yield of hydrogen and aromatics. Hydrogen formation, accompanied by aromatics, was not an exception, but a general phenomenon in the presence of V_2O_5/Al_2O_3. One possible way for high concentration of hydrogen was non-oxidative dehydrogenation, together with formation of aromatics. Carbon oxides were usually considered as deep oxidation products caused by surface adsorbed oxygen in oxidative dehydrogenation of light alkanes over vanadia or other metal oxide catalysts reported in [12,29,30]; however, decarboxylation and decarbonylation reactions might also be important sources for carbon oxide formation. Some proposed that lattice oxygen might result in olefin, carbon oxides or O-insertion products, depending on different activation mode by varying surface vanadia units and type of alkane reactant [13,14,19,31]. Activation of the weakest C–H bond in reactant molecule was supposed to be the initial step on the mixed catalysts, likely gave alkoxide or some other O-containing species as transition states or intermediates [13,14,32], these species could easily crack over acidic sites in P/HZSM-5/Kaolin under reaction conditions in our study, together with decarboxylation and decarbonylation, giving CO_2 and CO, respectively. Besides, addition of V_2O_5/Al_2O_3 decreased selectivity to ethane and ethylene, while improved selectivity to C_3 and C_4 products relatively. The above information suggested that introduction of V_2O_5/Al_2O_3 changed reaction pathways of n-heptane.

Table 3
Catalytic performances of catalysts after regeneration.

Catalysts		Before regeneration	After regeneration
Conversion, m%		58.34	57.19
Selectivity, %	H_2	0.99	0.84
	CH_4	0.86	0.82
	C_2H_6	3.07	3.16
	C_2H_4	4.99	5.03
	C_3H_8	10.99	10.54
	C_3H_6	16.47	16.73
	C_4H_{10}	4.95	4.69
	C_4H_8	8.38	8.27
	CO	1.39	1.31
	CO_2	2.02	2.13
	Arene	6.79	6.23

As V_2O_5/Al_2O_3 brought about significant effects in both conversion and product distribution, but the active sites in the V_2O_5/Al_2O_3 still needs further discussion. We noticed that, although the activity of Al_2O_3 alone was noticeably higher than V_2O_5/Al_2O_3 for conversion of n-heptane, the latter exhibited better activity than the former when mixed with the P/HZSM-5/Al_2O_3 catalyst. Therefore, we believed that the active sites must be related to vanadium species. The influences of reaction time on catalytic activity indicated that oxidized vanadia was the active site in V_2O_5/Al_2O_3, which can promote conversion of n-heptane; besides, activity of the used catalysts could almost be recovered after regeneration, giving further confirmation of the above inference. Reduction of vanadia by n-heptane under reaction condition might proceed during several quarters, but not instantly.

According to the obtained information, the reactions were concluded to proceed via the following pathways, as described in Fig. 6.

4. Conclusions

In this study, V_2O_5/Al_2O_3 was employed as lattice oxygen supplier and mixed with HZSM-5 catalyst for cracking of n-heptane evaluation. It was found that reduction of V^{5+} occurred and lattice oxygen was consumed in the reaction. Meanwhile, conversion of n-heptane increased from ~51% to ~59% and the mole ratio propylene and butylene to their corresponding alkanes also improved when substituting 20% of HZSM-5 catalyst with V_2O_5/Al_2O_3. However, their relative position, or reactant's contacting sequence with the two different catalysts, greatly influenced product distribution, and the results suggested that the reactant was favorable to be activated by V_2O_5/Al_2O_3 primarily before transferring to acidic sites of P/HZSM-5/Kaolin for further cracking. Besides, the influences of reaction time and regeneration strongly implied that the oxidized vanadia was the active sites in the V_2O_5/Al_2O_3, and the lattice oxygen provided by oxidized vanadia sites should be responsible for activation of n-heptane. Nevertheless, detailed activation mechanism by the V_2O_5/Al_2O_3 and reaction pathways on the mixed catalysts were obscure, and will be focused in a follow-up study.

Acknowledgements

We gratefully thank the staff of the Instrument Analysis Center at China University of Petroleum for their help in XRD, BET and FT-IR analyses.

References

[1] J.S. Buchanan, Catal. Today 55 (2000) 207.
[2] D.Z. Wang, Appl. Catal. A 141 (1996) N4.
[3] P.Q. Zhang, X.W. Guo, H.C. Guo, X.S. Wang, J. Mol. Catal. A 261 (2007) 139.
[4] C.Y. Li, C.H. Yang, H.H. Shan, Ind. Eng. Chem. Res. 46 (2007) 4914.
[5] P. O'Connor, A. Hakuli, P. Imhof, Stud. Surf. Sci. Catal. 149 (2004) 305.
[6] A. Aitani, T. Yoshikawa, T. Ino, Catal. Today 60 (2000) 111.
[7] M.A. den Hollander, M. Wissink, M. Makkee, J.A. Moulijn, Appl. Catal. A 223 (2002) 85.
[8] A. Corma, F.V. Melo, L. Sauvanaud, F.J. Ortega, Appl. Catal. A 265 (2004) 195.
[9] T. Ren, M. Patel, K. Blok, Energy 31 (2006) 425.
[10] H. Abrevaya, S.F. Abdo, R. Lyle Patton, US Patent 6 867 341 B1 (2005), to UOP LLC.
[11] X.B. Liu, W.Z. Li, H.O. Zhu, Q.J. Ge, Y.X. Chen, H.Y. Xu, Catal. Lett. 94 (2004) 31.
[12] H.W. Zanthoff, S.A. Buchholz, A. Pantazidis, C. Mirodatos, Chem. Eng. Sci. 54 (1999) 4397.
[13] P. Concepción, P. Botella, J.M. López Nieto, Appl. Catal. A 278 (2004) 45.
[14] G. Busca, Catal. Today 27 (1996) 457.
[15] R.M. Contractor, US Patent 4 668 802 (1987), to E. I. Du Pont de Nemours and Company.
[16] M. Abon, J.C. Volta, Appl. Catal. A 157 (1997) 173.
[17] G. Centi, S. Perathoner, F. Trifirb, Appl. Catal. A 157 (1997) 143.
[18] T. Shishido, T. Konishi, I. Matsuura, Y. Wang, K. Takaki, K. Takehira, Catal. Today 71 (2001) 77.
[19] T. Blasco, J.M. López Nieto, Appl. Catal. A 157 (1997) 117.
[20] H.H. Kung, M.C. Kung, Appl. Catal. A 157 (1997) 105.
[21] H.H. Kung, Adv. Catal. 40 (1994) 1.
[22] N. Steinfeldt, D. Müller, H. Berndt, Appl. Catal. A 272 (2004) 201.
[23] J.M. Kanervo, M.E. Harlin, A. Outi, I. Krause, M.A. Bañares, Catal. Today 78 (2003) 171.
[24] F. Klose, T. Wolff, H. Lorenz, A. Seidel-Morgenstern, Y. Suchorski, M. Piórkowska, H. Weiss, J. Catal. 247 (2007) 176.
[25] J. McGregor, Z. Huang, G. Shiko, L.F. Gladden, R.S. Stein, M.J. Duer, Z. Wu, P.C. Stair, S. Rugmini, S.D. Jackson, Catal. Today 142 (2009) 143.
[26] J. Haber, Catal. Today 142 (2009) 100.
[27] N. Rane, M. Kersbulck, R.A. van Santen, E.J.M. Hensen, Microporous Mesoporous Mater. 110 (2008) 279–291.
[28] K.K. Pant, D. Kunzru, Ind. Eng. Chem. Res. 36 (1997) 2059.
[29] K.D. Chen, A. Khodakov, J. Yang, A.T. Bell, E. Iglesia, J. Catal. 186 (1999) 325.
[30] O. Ovsitser, E.V. Kondratenko, Catal. Today 142 (2009) 138.
[31] R. Grabowski, Catal. Rev. 48 (2006) 199.
[32] G. Busca, E. Finocchioa, V. Lorenzelli, G. Ramis, M. Baldi, Catal. Today 49 (1999) 453.